Forecasting Tariff Rates and Enhancing Power Quality in Microgrids: The Synergistic Role of LSTM and UPQC

Satyabrata Sahoo
School of Electrical Engineering, KIIT Deemed to be University, India
satyabrata.sahoofel@kiit.ac.in

Sarat Chandra Swain
School of Electrical Engineering, KIIT Deemed to be University, India
scs_132@rediffmail.com

Ritesh Dash
School of EEE, REVA University, India
rdasheee@gmail.com

Padarbinda Samal
School of Electrical Engineering, KIIT Deemed to be University, India
padarbinda.samalfel@kiit.ac.in (corresponding author)

Received: 6 October 2023 | Revised: 25 October 2023 | Accepted: 28 October 2023

 DOI: https://doi.org/10.48084/etasr.6481

ABSTRACT

The current paper presents an original approach into the microgrid control framework by incorporating LSTM-based optimization with specific emphasis on refining the gain parameters of a Proportional-Integral-Derivative (PID) controller. This integration represents a significant advancement in improving the overall efficiency of microgrid control systems. By creatively applying LSTM optimization, the paper achieves dynamic adjustments of the PID controller's parameters, resulting in more precise regulation of output power quality. Through the utilization of the Unified Power Quality Conditioner (UPQC) in conjunction with LSTM-based optimization, the paper establishes a compelling link between improved power quality and the resultant tariff rates. This highlights their combined influence on enhancing power quality and calibrating tariff rates, providing a fresh perspective on optimizing microgrid operations.

Keywords formatting; microgrid; forecasting; LSTM; UPQC; power quality

I. INTRODUCTION

In an era characterized by increasing energy demands, growing awareness of environmental sustainability, and a desire for energy resilience, the concept of microgrids has emerged as a transformative solution for our evolving energy landscape. Microgrids represent a paradigm shift in the way we generate, distribute, and consume electrical energy [1-2]. Unlike traditional centralized power grids, which rely on large power plants and long-distance transmission lines, microgrids are localized, self-contained energy systems that serve specific communities, campuses, industrial facilities, or even individual buildings. The fundamental idea behind a microgrid is to decentralize and democratize energy generation and management. These self-sufficient energy ecosystems integrate a diverse mix of energy sources, including solar panels, wind turbines, Combined Heat and Power (CHP) systems, and energy storage technologies. Through advanced control systems and digital technologies, microgrids can intelligently balance supply and demand, optimize energy use, and seamlessly transition between grid-connected and islanded (standalone) modes [3-6].

The development of precise forecasting technologies is essential for successfully tackling the supply-demand complexities in contemporary energy management. These forecasts are segmented into specific time frames, to meet the precise energy management requirements of the microgrids. In the ultra-short term, which encompasses periods ranging from a few seconds to half an hour, the primary emphasis is placed on dynamic control for renewable power generators and load monitoring [7-8]. Real-time adjustments are employed to optimize the operation of renewable energy sources, taking into

account sudden weather shifts and fluctuations in energy demand, thus ensuring efficient performance.

The current research takes a comprehensive approach to improve tariff rate forecasting within microgrids by integrating Unified Power Quality Conditioner (UPQC) technology and Long Short-Term Memory (LSTM) Neural Networks (NNs) [9-10]. Additionally, it explores the effects of UPQC on enhancing power quality and examines the utilization of LSTM-based forecasting models in microgrid applications. The process of collecting data encompasses the gathering of historical load data, tariff rates, and power quality parameters at the Point of Common Coupling (PCC) from actual microgrid systems in the field or through the use of simulation tools. Furthermore, an evaluation will be conducted within a microgrid simulation environment to assess the UPQC device's performance in reducing voltage sags, swells, and harmonics, with the ultimate goal of enhancing power quality. By integrating UPQC into the tariff rate forecasting model, we not only enhance the precision of our predictions but also address the real-time power quality challenges that can impact microgrid operations [11]. This fusion of technologies promises more reliable energy management and decision-making within microgrids, ensuring that they can adapt to dynamic supply and demand conditions while maintaining optimal power quality standards [12].

II. LSTM MODEL AND ANALYSIS

LSTM represents a specialized category of Recursive Neural Networks (RNNs). At the heart of the LSTM RNN lies the cell state, a crucial component designed to preserve information over extended periods. Only a fraction of the stored information actively participates in linear interactions [13]. The fundamental operations within the LSTM NN revolve around three gates: the forget gate, the input gate, and the output gate. These gates predominantly consist of a Sigmoid layer and a multiplication operation. The primary functionality materializes when these gates govern the processing of information within the cell state [14]. Through the judicious control of the forget gate, input gate, and output gate, the LSTM NN adeptly manages and sustains the information stored in the cell state—a pivotal role within the LSTM architecture [15-17]. In addition to the three gates, the LSTM cell incorporates a crucial mechanism known as the cell update. Typically implemented through a hyperbolic tangent (tanh) layer, this update mechanism plays an indispensable role in the LSTM's ability to assimilate and preserve new information in its long-term memory. The cell update mechanism enables the LSTM to adapt and learn from incoming data over time. The proposed LSTM architecture for PID controller tuning is shown in Figure 1. The proposed approach involves the utilization of an LSTM-based method for dynamically adjusting the gain of a PID controller. This adjustment is achieved through the processing of direct and quadrature axis currents. LSTMs are renowned for their capability to handle long-term dependencies in sequential data, making them well-suited for capturing intricate temporal patterns in control system currents. In this context, the LSTM architecture has been thoughtfully designed to take direct and quadrature axis currents as inputs and generate the optimal PID controller gain as the output. The training of the LSTM model has been carried out using a comprehensive data set comprising paired direct and quadrature axis currents along with their corresponding PID controller gains. In real-time applications, the trained LSTM model is employed to predict the most suitable PID gain based on the current values received from the system. This dynamic and adaptive tuning mechanism empowers the PID controller to continuously adjust its gain in response to changing operating conditions and system dynamics. The flow chart for LSTM based cost analysis and forecasting model is shown in Figure 2.

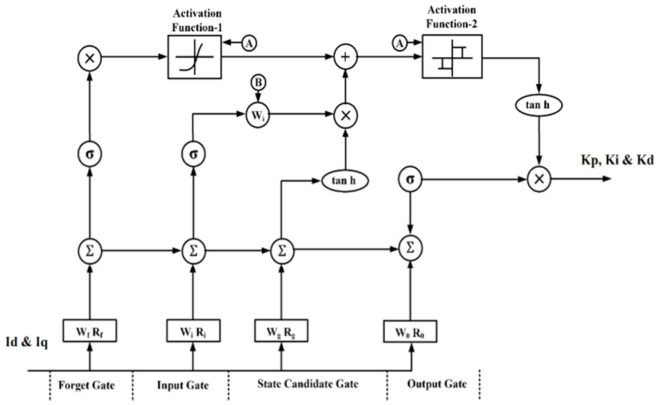

Fig. 1. The proposed LSTM architecture for PID controller tuning.

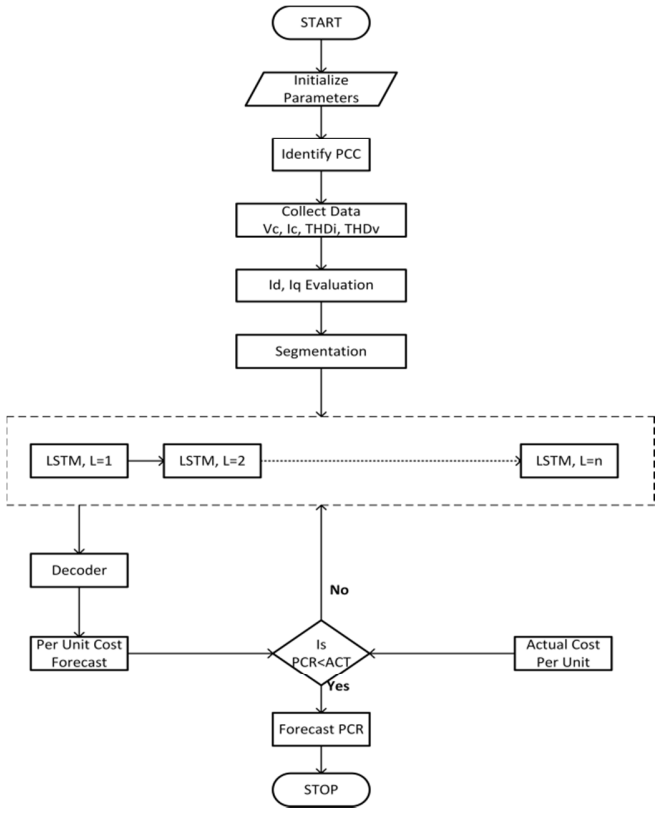

Fig. 2. LSTM-based per unit cost analysis and forecasting in a microgrid.

III. SIMULATION SET UP

The model experimental setup for tuning a PID controller based on the LSTM model is shown in Figure 4. The proposed LSTM model initiates its operation by capturing several microgrid parameters, including three-phase voltage and three-phase current at the point of common coupling. To facilitate coordinated control actions for the UPQC, all grid-level three-phase parameters are first transformed into DQ parameters and then further converted from the DQ reference frame to the alpha-beta reference frame [18-19]. To maintain the conversion ratio within the specified boundaries, a hysteresis competitive controller is implemented in front of the alpha-beta lines. This is followed by the consideration of 8 different state variable conditions that determine the magnitude level required for the activation function within the LSTM algorithm. Three distinct states of the LSTM model are designed, taking into account 24 state variables that ultimately influence the output layer of the proposed model. To bridge the gap between machine-level language and encoding, an embedding layer is provided in conjunction with backward memory allocation, enabling the retrieval of correlations between input parameters and predicted parameters. The output layer in the proposed model is a function of various state variables, necessitating the inclusion of two additional decoders: one for the recurrent layer and another for the output layer.

Table I presents a detailed examination of the LSTM model parameters employed within the SARIMA+RMSprop framework for time series forecasting. The input size is configured as 4, encompassing both direct and quadrature axis components in a bid to effectively process and analyze the pertinent time series data. With 10 hidden units, the LSTM model balances between complexity and computational efficiency, effectively capturing essential patterns in the data. To handle intricate temporal dependencies, the model is furnished with 4 LSTM layers, although it should be noted that this configuration may necessitate more data and training time. The activation function for the LSTM input layers is thoughtfully chosen as a combination of sigmoid and tanh, while the output layer adopts the sigmoid function, thereby facilitating prediction tasks and generating continuous output values within a specific range. The learning rate is set to 0.01, striking an optimal balance between fine-tuning the model's weights during the gradient descent optimization process and avoiding large weight updates that may hinder convergence. The RMSprop optimization method was chosen for its adaptive learning rate mechanism based on gradient history, leading to faster convergence and effective optimization within the SARIMA framework. To ensure training efficiency, a batch size of 50 is selected, optimizing memory usage and computational speed during the training process. To achieve convergence and optimal weight adjustments, the model undergoes training for 200 epochs, providing sufficient iterations for the LSTM to capture essential patterns in the time series data.

Gaussian gradient analysis is a valuable technique used to study the behavior of activation functions in relation to specific input points, providing insights into their sensitivity to changes in input values and revealing their characteristics within targeted regions.

TABLE I. LSTM PARAMETERS

Parameter	Magnitude	Remark
Input size	4	Two sets of direct and quadrature axis components
Hidden inputs	10	Determines problem complexity
Number of layers	4	More layers can capture complex patterns but may require more data and training time
Activation function	Sigmoid and tanh	Output layer prediction
Dropout rate	0.1	Regularization to prevent overfitting
Recurrent dropout	0.2	Regularization of LSTM layers
Learning rate	0.01	Adjusting the step size for gradient descent
Optimization	-	SARIMA+RMSprop
Batch size	50	Memory usage and computational efficiency
Epochs	200	Iterations for convergence
Loss function	-	Mean Squared Error (MSE)

In Figures 3(a)-(b), two distinct activation functions, AF1 and AF2, are thoroughly investigated. The Figures visually depict the gradients of these activation functions at predefined input points. The gradients for AF1 are meticulously calculated at -0.03 and 0.03, while for AF2, the analysis focuses on -0.021 and 0.021. Figure 3(b) reveals intriguing findings. The algorithm demonstrates heightened sensitivity to changes in boundary value conditions, particularly concerning the type and magnitude of Total Harmonic Distortion (THD) present at the PCC. The model achieves its optimal performance when subjected to a maximum deviation of 8.7% in step during transient disturbances with respect to gain.

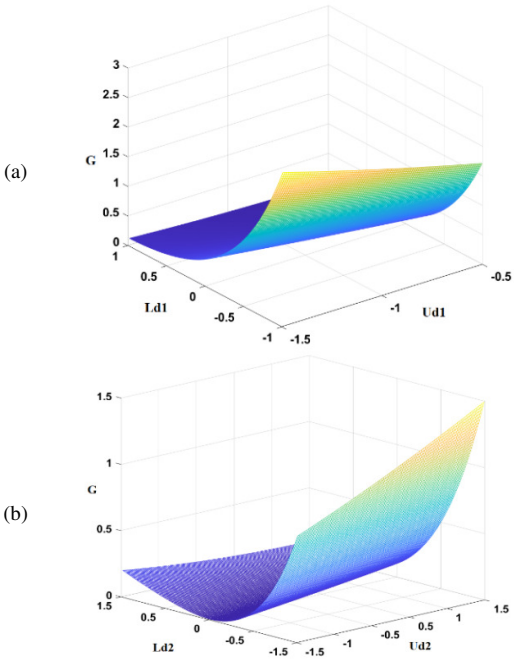

Fig. 3. Gaussian Gradient Analysis with (a) AF1 = [-0.03 0.03] and (b) AF2= [-0.021 0.021].

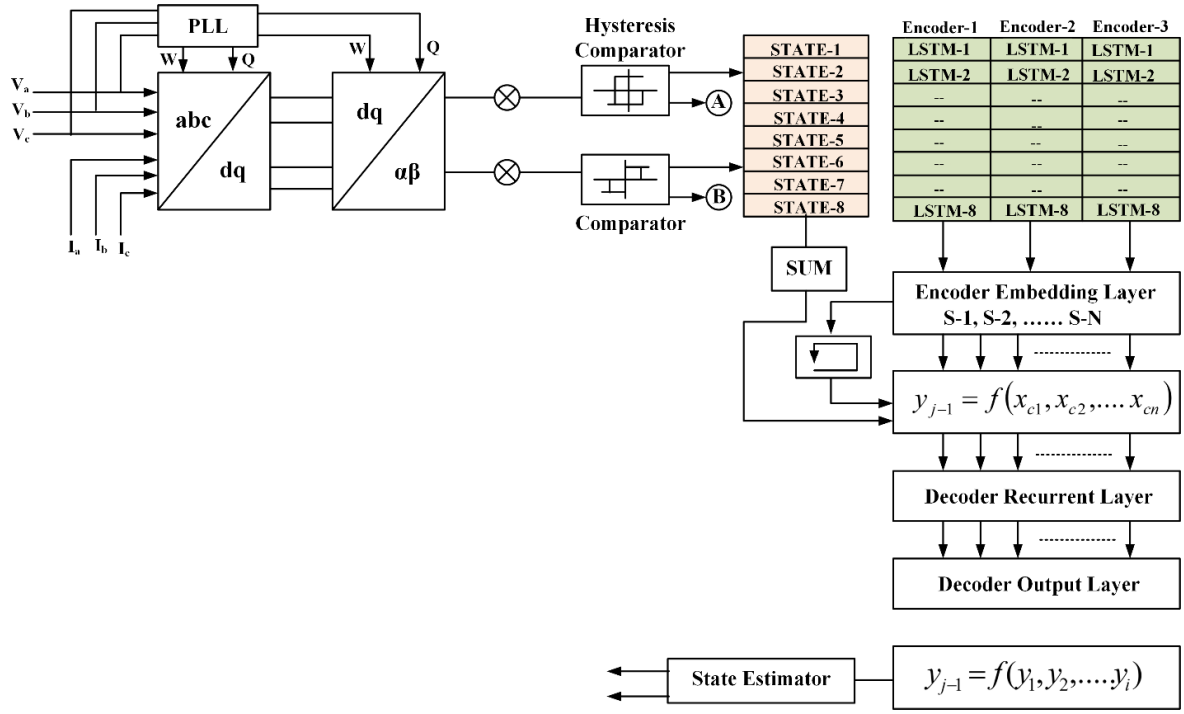

Fig. 4. Experimental setup model for PID controller tuning using LSTM.

IV. RESULT ANALYSIS AND DISCUSSION

In order to process the proposed controller, the designed microgrid has a capacity of 10 kW [20]. The designed microgrid consists of a solar photovoltaic (PV) system of 3 kW and wind system of 4 kW, and a fuel cell of 3 kW. Modeling of PV cells is required for an efficient design of a PV system. First, the performance of the microgrid has been analyzed with the conventional PID controller and a forecasting model has been designed using the SARIMA method. Then the parameters of the PID controller were fine-tuned by the LSTM RNN while UPQC was integrated with the microgrid and the performance is analyzed.

A comparative analysis between the LSTM and PID controllers presenting the findings is shown at Table II. Firstly, the proportional gain is assessed, which reflects the proportional control behavior of these controllers. The PID controller exhibits a proportional gain of 0.32, while the LSTM-controller displays a lower value of 0.21. This disparity suggests that the LSTM controller responds more conservatively to fluctuations in the error signal compared to the PID controller. The PID controller manifests an integral gain of 0.47, whereas the LSTM controller demonstrates a diminished value of 0.27. This discrepancy indicates that the LSTM controller is less prone to cumulative errors over time, resulting in more stable control over prolonged deviations. The PID controller boasts a derivative gain of 0.05, while the LSTM controller showcases a smaller value of 0.038. This reduced derivative gain in the LSTM controller signifies a smoother response to rapid changes, mitigating the risk of overshooting or oscillations. Additionally, we explore sampling time, which represents the time interval between successive control actions. The PID controller employs a sampling time of 0.01 s, whereas the LSTM controller adopts a significantly faster sampling time of 0.001 s. This enhanced sampling rate equips the LSTM controller to respond with greater agility to dynamic system alterations, thereby enhancing its real-time control capabilities. The reduced error and standard deviation values of the LSTM controller indicate its superior accuracy and precision in achieving the desired control objectives.

TABLE II. CONTROLLER GAIN COMPARATIVE ANALYSIS

Parameter	PID controller	LSTM controller
Proportional gain	0.32	0.21
Integral gain	0.47	0.27
Derivative	0.05	0.038
Sampling time	0.01 s	0.001 s
Error	17.22%	8.07%
Std Deviation	1.652	0.69

Table III presents a comprehensive comparative analysis of the loading performance of the LSTM-SARIMA-PID Controller under different loading conditions. The analysis evaluates essential parameters, including PCC-THD-Current, PCC-THD-Voltage, frequency variation, and transient voltage rise, to assess the controller's performance across varying load levels. Table IV presents a comprehensive comparative analysis of the PID-SARIMA and LSTM-SARIMA forecasting models, focusing on their economic forecasting performance under different loading conditions. The Table provides valuable insights into the accuracy and reliability of these models by comparing their actual and forecasted tariff values. Starting with the 10% full load scenario, PID-SARIMA records an actual tariff value of 4.06, while its forecasted value is slightly lower at 3.92. In contrast, LSTM-SARIMA impressively predicts the actual tariff with a forecasted value of 3.97,

indicating its precision in economic forecasting at this load level. Similarly, the tariff forecasting has been done at other loading conditions.

TABLE III. LOADING PERFORMANCE ANALYSIS

Loading (% of full load)	PCC-THD-Current	PCC-THD-Voltage	Frequency variation	Transient voltage rise
10	4.02	2.33	0.54	0.06
30	4.70	2.93	0.63	0.07
45	5.56	3.40	0.73	0.08
60	6.59	3.95	0.84	0.10
75	8.18	4.78	1.02	0.12
90	8.60	4.97	1.06	0.12
100	8.79	4.96	1.06	0.12

TABLE IV. COMPARATIVE ANALYSIS BETWEEN ACTUAL AND FORECASTED TARIFFS

Loading (% of full load)	PID-SARIMA		LSTM-SARIMA	
	Tariff		Tariff	
	Actual	Forecasted	Actual	Forecasted
10	4.06	3.92	3.97	3.97
30	4.64	4.66	4.73	4.73
45	5.36	5.55	5.63	5.63
60	6.18	6.61	6.70	6.69
75	7.12	7.87	7.97	7.97
90	8.56	9.37	9.48	9.48
100	10.05	11.15	11.29	11.28

TABLE V. COMPARATIVE ANALYSIS BETWEEN ACTUAL AND FORECASTED PRICE BETWEEN PID-SARIMA AND LSTM-SARIMA BASED ON THE CURRENT THD LEVEL

PCC-THD-Current	PID-SARIMA		LSTM-SARIMA	
	Tariff		Tariff	
	Actual	Forecasted	Actual	Forecasted
4.02	4.04	3.89	3.99	3.96
4.70	4.80	4.63	4.75	4.71
5.56	5.71	5.51	5.65	5.61
6.59	6.80	6.55	6.72	6.67
8.18	8.09	7.80	8.00	7.94
8.60	9.64	9.28	9.52	9.45
8.79	11.48	11.04	11.33	11.24

TABLE VI. COMPARATIVE ANALYSIS BETWEEN ACTUAL AND FORECASTED PRICE BETWEEN PID-SARIMA AND LSTM-SARIMA BASED ON THE VOLTAGE THD LEVEL

PCC-THD-Voltage	PID-SARIMA		LSTM-SARIMA	
	Tariff		Tariff	
	Actual	Forecasted	Actual	Forecasted
2.33	3.80	3.59	3.62	3.62
2.93	4.52	4.28	4.31	4.30
3.40	5.37	5.09	5.13	5.12
3.95	6.40	6.06	6.10	6.09
4.78	7.61	7.21	7.26	7.25
4.97	9.07	8.58	8.64	8.63
4.96	10.80	10.21	10.28	10.27

In Table V, a comprehensive comparison is presented between the actual and forecasted prices derived from PID-SARIMA and LSTM-SARIMA models. This analysis specifically focuses on varying THD levels to calculate the corresponding price per unit of energy. The results are illuminating and provide valuable insights into the efficiency of these models under different THD conditions. For instance, when the THD level is at 4.02, the forecasted tariff using LSTM-SARIMA stands at 3.96, whereas the PID-SARIMA model yields a tariff of 3.89. This signifies a notable increase in revenue, with the LSTM-SARIMA model generating at least 1.79% more revenue per unit of energy compared to the PID-SARIMA model. These findings emphasize the superior predictive power of LSTM-SARIMA in this scenario. Furthermore, at the highest observed THD level of 11.48, the LSTM-SARIMA model predicts a tariff rate of 11.24, while the PID-SARIMA model forecasts a rate of 11.04. This stark contrast clearly demonstrates the efficiency of the proposed LSTM-SARIMA model. Even under challenging conditions with elevated THD levels, the LSTM-SARIMA model consistently outperforms the traditional PID-SARIMA model, ensuring a higher per-unit forecast. Importantly, this analysis takes into account the Aggregate Technical and Commercial (AT&C) losses, providing a holistic view of the forecasting models' performance. Considering the inclusion of AT&C losses, the superiority of the LSTM-SARIMA model in providing accurate and profitable energy price forecasts becomes even more evident.

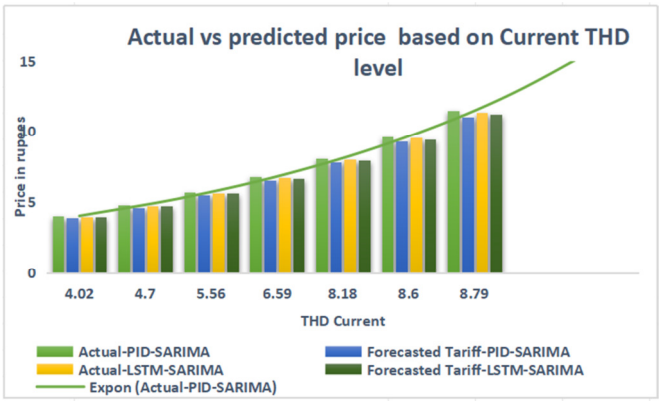

Fig. 5. Price forecasted by PID-SARIMA and LSTM-SARIMA.

In Table VI, a detailed comparative analysis is presented, focusing on the actual and forecasted prices under varying Voltage THD levels. This examination is critical due to the significant impact voltage fluctuations and distortions can have on energy distribution systems. One specific scenario worth noting is when the voltage THD level is measured at 4.96. Under these conditions, the LSTM-SARIMA model predicts a tariff rate of 10.27 units, whereas the PID-SARIMA model forecasts a rate of 10.21 units. This subtle yet consistent difference underscores the LSTM-SARIMA model's ability to provide more accurate predictions, even when voltage THD levels are moderately elevated. Such precision is crucial for energy providers, ensuring a stable and reliable electricity supply to consumers. It is essential to highlight that the analysis in Table VI adheres strictly to the standards outlined by the IEEE-519, a universally acknowledged benchmark in the energy industry. By referencing this standard, the efficacy of the proposed LSTM-SARIMA model as a controller becomes evident. This comprehensive analysis emphasizes the significance of considering voltage-related factors in energy

forecasting models, showcasing the LSTM-SARIMA model's superiority over PID-SARIMA, especially in situations involving moderate voltage THD levels.

It is seen that as the current and voltage THD increases, the energy tariff also increases. But with the LSTM-SARIMA model, the price fluctuations are less than when using the PID-SARIMA model. The actual vs predicted price by PID-SARIMA model and LSTM-SARIMA model are shown in Figure 5, where we can observe an increase in actual and forecasted price as the THD in current increases.

V. CONCLUSION

In conclusion, the utilization of LSTM-based forecasting models for predicting microgrids' per unit tariff has demonstrated significant promise in producing accurate and dependable forecasts. These models excel in capturing intricate temporal patterns and dependencies within data, enabling precise predictions of forthcoming tariff rates. Nonetheless, it is essential to recognize that the performance of LSTM models is heavily reliant on the availability and quality of data. Suboptimal or noisy data can adversely affect prediction accuracy. Hence, ensuring the quality and accessibility of data is paramount for the effective deployment of LSTM-based forecasting in microgrid tariff prediction. Hence, in this paper, the LSTM-SARIMA model with UPQC has been proven to be a better forecasting model than the conventional PID-SARIMA model.

REFERENCES

[1] S. A. Alavi, K. Mehran, V. Vahidinasab, and J. P. S. Catalão, "Forecast-Based Consensus Control for DC Microgrids Using Distributed Long Short-Term Memory Deep Learning Models," *IEEE Transactions on Smart Grid*, vol. 12, no. 5, pp. 3718–3730, Sep. 2021, https://doi.org/10.1109/TSG.2021.3070959.

[2] D. Kumar, H. D. Mathur, S. Bhanot, and R. C. Bansal, "Forecasting of solar and wind power using LSTM RNN for load frequency control in isolated microgrid," *International Journal of Modelling and Simulation*, vol. 41, no. 4, pp. 311–323, Jul. 2021, https://doi.org/10.1080/02286203.2020.1767840.

[3] A. A. Muzumdar, C. N. Modi, M. G. M, and C. Vyjayanthi, "Designing a Robust and Accurate Model for Consumer-Centric Short-Term Load Forecasting in Microgrid Environment," *IEEE Systems Journal*, vol. 16, no. 2, pp. 2448–2459, Jun. 2022, https://doi.org/10.1109/JSYST.2021.3073493.

[4] W. Kong, Z. Y. Dong, Y. Jia, D. J. Hill, Y. Xu, and Y. Zhang, "Short-Term Residential Load Forecasting Based on LSTM Recurrent Neural Network," *IEEE Transactions on Smart Grid*, vol. 10, no. 1, pp. 841–851, Jan. 2019, https://doi.org/10.1109/TSG.2017.2753802.

[5] J. Li *et al.*, "A Novel Hybrid Short-Term Load Forecasting Method of Smart Grid Using MLR and LSTM Neural Network," *IEEE Transactions on Industrial Informatics*, vol. 17, no. 4, pp. 2443–2452, Apr. 2021, https://doi.org/10.1109/TII.2020.3000184.

[6] T. Wang, D. O'Neill, and H. Kamath, "Dynamic Control and Optimization of Distributed Energy Resources in a Microgrid," *IEEE Transactions on Smart Grid*, vol. 6, no. 6, pp. 2884–2894, Aug. 2015, https://doi.org/10.1109/TSG.2015.2430286.

[7] X. Cao, S. Dong, Z. Wu, and Y. Jing, "A Data-Driven Hybrid Optimization Model for Short-Term Residential Load Forecasting," in *2015 IEEE International Conference on Computer and Information Technology; Ubiquitous Computing and Communications; Dependable, Autonomic and Secure Computing; Pervasive Intelligence and Computing*, Liverpool, UK, Jul. 2015, pp. 283–287, https://doi.org/10.1109/CIT/IUCC/DASC/PICOM.2015.41.

[8] T. Ergen and S. S. Kozat, "Online Training of LSTM Networks in Distributed Systems for Variable Length Data Sequences," *IEEE Transactions on Neural Networks and Learning Systems*, vol. 29, no. 10, pp. 5159–5165, Jul. 2018, https://doi.org/10.1109/TNNLS.2017.2770179.

[9] J. Xie, R. Yang, H. B. Gooi, and H. D. Nguyen, "PID-based CNN-LSTM for accuracy-boosted virtual sensor in battery thermal management system," *Applied Energy*, vol. 331, Feb. 2023, Art. no. 120424, https://doi.org/10.1016/j.apenergy.2022.120424.

[10] H. Jahangir, H. Tayarani, S. S. Gougheri, M. A. Golkar, A. Ahmadian, and A. Elkamel, "Deep Learning-Based Forecasting Approach in Smart Grids With Microclustering and Bidirectional LSTM Network," *IEEE Transactions on Industrial Electronics*, vol. 68, no. 9, pp. 8298–8309, Sep. 2021, https://doi.org/10.1109/TIE.2020.3009604.

[11] D. El Bourakadi, A. Yahyaouy, and J. Boumhidi, "Intelligent energy management for micro-grid based on deep learning LSTM prediction model and fuzzy decision-making," *Sustainable Computing: Informatics and Systems*, vol. 35, Sep. 2022, Art. no. 100709, https://doi.org/10.1016/j.suscom.2022.100709.

[12] M. Mohamed, F. E. Mahmood, M. A. Abd, A. Chandra, and B. Singh, "Dynamic Forecasting of Solar Energy Microgrid Systems Using Feature Engineering," *IEEE Transactions on Industry Applications*, vol. 58, no. 6, pp. 7857–7869, Aug. 2022, https://doi.org/10.1109/TIA.2022.3199182.

[13] X. Lin, R. Zamora, C. A. Baguley, and A. K. Srivastava, "A Hybrid Short-Term Load Forecasting Approach for Individual Residential Customer," *IEEE Transactions on Power Delivery*, vol. 38, no. 1, pp. 26–37, Oct. 2023, https://doi.org/10.1109/TPWRD.2022.3178822.

[14] S. Sahoo, S. Swain, R. Dash, P. Sanjeevikumar, K. Jyotheeswara Reddy, and V. Subburaj, "Novel Gaussian flower pollination algorithm with IoT for unit price prediction in peer-to-peer energy trading market," *Energy Reports*, vol. 7, pp. 8265–8276, Nov. 2021, https://doi.org/10.1016/j.egyr.2021.08.170.

[15] S. Sahoo, S. Chandra Swain, and R. Dash, "A Novel Flower Pollination Method for Unit Price Estimation in a Microgrid," in *2022 3rd International Conference for Emerging Technology (INCET)*, Belgaum, India, Feb. 2022, https://doi.org/10.1109/INCET54531.2022.9824553.

[16] V. P. Rajderkar and V. K. Chandrakar, "Design Coordination of a Fuzzy-based Unified Power Flow Controller with Hybrid Energy Storage for Enriching Power System Dynamics," *Engineering, Technology & Applied Science Research*, vol. 13, no. 1, pp. 10027–10032, Feb. 2023, https://doi.org/10.48084/etasr.5508.

[17] V. H. Nguyen, H. Nguyen, M. T. Cao, and K. H. Le, "Performance Comparison between PSO and GA in Improving Dynamic Voltage Stability in ANFIS Controllers for STATCOM," *Engineering, Technology & Applied Science Research*, vol. 9, no. 6, pp. 4863–4869, Dec. 2019, https://doi.org/10.48084/etasr.3032.